Division and Fusion, Extension, Adhesion, and Retraction of Vesicles Created through Langmuir Monolayer Collapse: Cell-like Behavior

E. Hatta*

Nanoelectronics Laboratory, Graduate School of Information Science and Technology, Hokkaido University, Sapporo, 060-0814 Japan

Received: March 19, 2007; In Final Form: June 25, 2007

The motion of vesicles created through Langmuir monolayer collapse has been investigated. The vesicles grow only in a narrow molecular area range, and they exhibit remarkable, various biological cell-like behaviors such as division (cell division in cell biology, cytokinesis) and self-propulsion (motility). The vesicle division includes some dynamic modes: (i) an expulsion of a single satellite vesicle from an initial vesicle, (ii) a hierarchical and a sequential expulsion of a satellite vesicle, and (iii) a successive expulsion of two satellite vesicles from an initial vesicle. Two neighboring vesicles often show alternate fusion and division between them. Strong shape fluctuations dominate through vesicle division. The vesicles created exhibit distinct motions depending on the molecular area. At a large molecular area where most initial vesicles are created, they show a continuous, random motion on a few tens of micrometers length scale with a strong shape fluctuation and a constant velocity fluctuation profile. At a small molecular area they cease to move and shape fluctuations also become suppressed. At an intermediate molecular area there coexist vesicles with different dynamic modes: some vesicles show random motion similar to that at a large molecular area, but in a less fluctuating manner, while others exhibit a directional motion with an intermittent velocity jump. The directional motion is characterized by three distinct steps, i.e., extension, adhesion, and retraction. The characteristic motion is discussed from the viewpoint of haptotaxis, or the motion driven by adhesion gradients on the monolayer created by the local transfer of charged surfactant molecules between the vesicle and the monolayer, which the vesicle adheres to.

Introduction

In a monolayer at the air−water interface (Langmuir monolayer) besides transitions between two-dimensional phases there exists another class of transition between two and three dimensions (*collapse transition*) at a sufficiently strong lateral surface pressure beyond which the monolayer cannot be compressed further. Collapse transitions have received much attention from physical, chemical, and biological aspects, and various intriguing collapsed structures have been found, including twisted ribbons,[1,2] buckling,[3,4] straight[5,6] and giant[6,7] folds, and vesicles[5] on micrometer-length scales. The monolayer often releases the stress on the molecular-length scale, causing breakage.[8,9] The motion of the above soft collapsed structure is *passive* in that it moves under the application of external force such as a viscous force from its surrounding medium after it protrudes into the subphase. Dynamic properties of a biological cell as an *active* object, on the other hand, have been studied extensively.[10,11] One of the most important research areas in this subject concerns the mechanisms that are adopted by living cells. Cells exhibit complex morphological changes such as growth, fusion, budding, and fission to achieve basic cellular functions. Moreover, cells must exert various forces in biological bodies (i) to move organelles and vesicles within the cytoplasm, (ii) to separate chromosomes in mitosis, (iii) to separate into two daughter cells from a mother cell in cytokinesis, (iv) in cell migration phenomena, and (v) in modifying their environment, particularly the extracellular matrix.[12] Of these, in cell migration it is important to understand how cells employ the various force-generating processes to move across a surface. Migration of all cells across substrates involves a complex, dynamic interplay between extension, adhesion, and retraction. A moving keratinocyte and a moving fibroblast, for instance, display the same sequence of changes in cell morphology. The adhesion plays two significant roles in the whole process of cell migration: it anchors the cell to the substrate and it prevents the leading edge from retracting. In the last step of the movement, the rear of the cell is *pulled forward*, breaking its adhesions to the substrate (de-adhesion). The tail of the cell is often seen to snap loosely from its adhesion sites, probably by its elastic tension. The adhesion of the leading edge of the cell is crucial for successive extension, leading to tension development followed by retraction. The study of forces required for the cell movement is thus essential for the understanding of cell migration and adhesion.

In our present study the monolayer collapses on a buffered alkaline subphase by solubilization of monolayer material into the subphase, creating highly active vesicles. They exhibit intriguing cell-like, spontaneous behaviors. They are classified into two main groups. The first one is vesicle division and fusion, and the second is vesicle migration. The former includes some dynamic modes: (i) an expulsion of a satellite vesicle from an initial vesicle, (ii) a hierarchical and a sequential expulsion of a vesicle, (iii) a successive expulsion of two satellite vesicles from an initial vesicle, and (iv) an alternate fusion and division between two neighboring vesicles. The second one is typified by (i) a random motion with a constant velocity fluctuation and (ii) a directed motion with an intermittent

* E-mail: hatta@nano.ist.hokudai.ac.jp.

10.1021/jp0721649 CCC: $37.00
Published on Web 08/09/2007

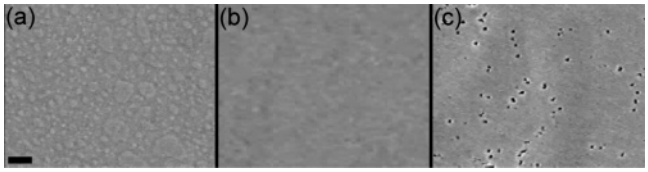

Figure 1. Phase contrast microscopy images of an octadecanoic acid monolayer at some molecular areas. The subphase temperature is 20 °C and the subphase pH is 8.0. (a) $A = 0.674$ nm^2/molecule, (b) $A = 0.259$ nm^2/molecule, and (c) $A = 0.254$ nm^2/molecule. The scale bar length is 50 μm.

velocity jump profile. In the intermittent, directed motion the vesicle clearly moves forward by three definite steps: (i) *extension* of the vesicle, (ii) *adhesion* of the front part of the vesicle to the monolayer, and (iii) *retraction* of the rear part of the vesicle (preceded by its de-adhesion from the monolayer). The complex motion of vesicles observed is considered from the viewpoint of *haptotaxis*, or the motion driven by the adhesion (wettability) gradient at the location of the vesicle produced by the local transfer of charged molecules between the vesicle and the monolayer.

Experimental Section

Monolayers of octadecanoic acid [stearic acid, C18, 99% pure, Sigma Chemicals] dissolved in 0.5 mM chloroform (97% pure, Kanto Chemicals) were spread onto a liquid subphase (Millipore Mill-Q system filtered water, 18.0 MΩ cm). All experiments were performed at 20.0 ± 0.2 °C. The pH values of the subphase from 6.0 to 8.0 were adjusted with $NaHCO_3$. These materials were used without further purification. We observed the creation of vesicles followed by their division and self-propelled motion only at the highest subphase pH value under investigation, i.e., at pH 8.0, and in a narrow molecular area range (0.238−0.254 nm^2/molecule). Below we thus show the results on monolayer collapse at pH 8.0 only. It has been established that phase contrast microscopy (PCM) provides a powerful tool for following collapse morphologies and their dynamics of monolayers protruding from the water surface.[9] A PCM image is a projection of the vesicles extending as much as a few tens of micrometers into the subphase. Created vesicles were monitored using phase contrast microscopy (NIKON, OPTIPHOT-2) equipped with a CCD camera (Hamamatsu, C2400-77H) followed by an image processor (Hamamatsu, DVS-3000). The incident light was transmitted through the bottom of a home-made glass trough placed on the microscope stage. The motion of vesicles was recorded at a frequency of 30 frames/s while constantly monitoring the $\pi-A$ isotherms with a Wilhelmy plate balance. The width of the trough used was 10 cm, and the monolayers were compressed at a fixed low rate of 1.66×10^{-5} m^2/s to diminish the kinetic effects of lateral compression. Larger immobile vesicles and other collapsed structures were used as reference points to follow the uniform collective motion of the monolayer. Subtracting it from the vesicles' motion leaves only their active motion. From the corrected position data, the trajectories of the vesicles and the velocity profiles were determined.

Results

In Figure 1 we show some typical PCM images of an octadecanoic acid monolayer at $T = 20$ °C and pH 8.0. At the largest area ($A = 0.674$ nm^2/molecule, Figure 1a), it can be seen from the image that the fatty acid molecules already exist as molecularly assembled islands with a domain structure

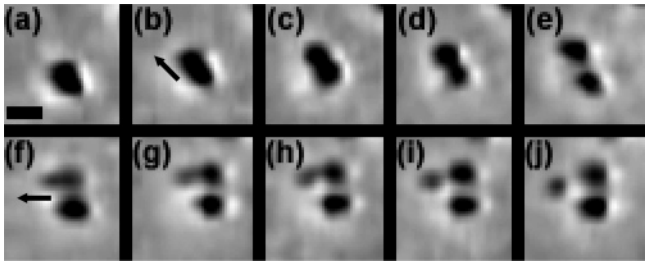

Figure 2. Phase contrast microscopy images of a hierarchical expulsion of a child vesicle from a mother vesicle ($A = 0.246$ nm^2/molecule). Elapsed times are (a) 0, (b) 0.27, (c) 0.72, (d) 0.8, (e) 1.2, (f) 1.86, (g) 2.07, (h) 2.1, (i) 2.13, and (j) 2.25 s. The scale bar length is 10 μm.

surrounded by bare water immediately after spreading the solution. This suggests that the molecules exert attractive forces among themselves that are strong enough to cause spontaneous assembly of the molecules on water under this condition, instead of an ideal gas (G) phase where the molecules can move freely. As the area decreases, those domains coalesce with each other, forming uniform larger domains (Figure 1b). After the coalescence of domains is completed throughout the water surface, at a certain surface area ($A = 0.254$ nm^2/molecule) the monolayer starts to collapse by solubilization of material from the monolayer into the subphase, creating many vesicles (seen as black spots, Figure 1c). The number of vesicles increases monotonically by the creation of new vesicles as well as the division of existing vesicles as the surface area decreases. Finally, the monolayer collapses via the second collapse mode or the formation of large-scale soft collapsed structures as giant lamellar ones where vesicles still remain below the monolayer. Below we focus our attention on the dynamics of vesicles observed only in a narrow surface molecular area range ($A = 0.238-0.254$ nm^2/molecule).

The vesicles created are not immobile below the monolayer but show highly active behaviors. They exhibit topological shape transitions such as division and fusion of vesicles as well as two-dimensional self-propulsive motions. First we show several distinct modes for the division of vesicles. The hierarchical sequence of vesicle division is shown in Figure 2. The original, mother vesicle buds and expels a satellite, child vesicle (Figure 2a−e), and the second, expelled vesicle again buds and expels the third vesicle subsequently (Figure 2f−j). Throughout this division process the shape of each vesicle is fluctuating strongly all the time. The satellite vesicle is fluctuating particularly strongly immediately after expulsion from the mother vesicle. Another mode of vesicle division is shown in Figure 3. A mother vesicle expels two child vesicles successively in this case. The vesicles often exhibit fusion as well as division (Figure 4). The fusion between vesicles occurs more often between strongly fluctuating, neighboring vesicles. The vesicles show not only topological shape transitions such as division and fusion but also intriguing two-dimensional self-propelled motions. In Figure 5 we show two types of velocity profiles of self-propelled vesicles. The velocity profile of Figure 5a shows a constant velocity fluctuation during the motion of the vesicle (type a), while the Figure 5b velocity profile shows intermittent velocity jumps between constant velocity fluctuations (type b). The motions of vesicles with such two types of velocity profiles are shown in Figures 6 and 7, respectively. In Figure 6 the initial vesicle expels a small satellite vesicle (Figure 6a−c) after its budding. The expelled vesicle migrates in a continuous manner, accompanied by a strong shape fluctuation. Figure 7 shows a highlighted process observed in the motion of the vesicle with the type b velocity profile. The front part of the vesicle extends

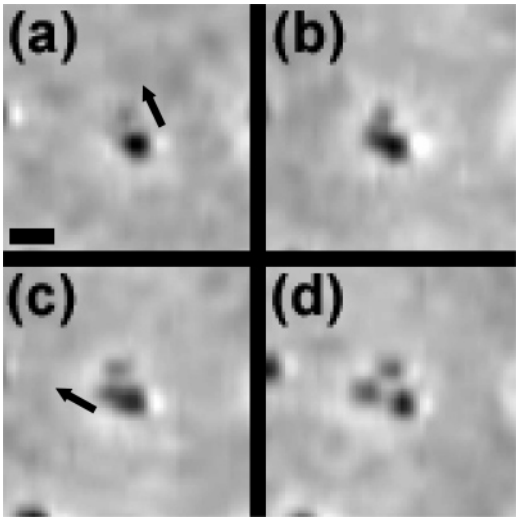

Figure 3. Phase contrast microscopy images of a successive expulsion of two satellite vesicles from an initial vesicle (A = 0.247 nm^2/molecule). Elapsed times are (a) 0, (b) 0.24, (c) 0.3, and (d) 0.42 s. The scale bar length is 10 μm.

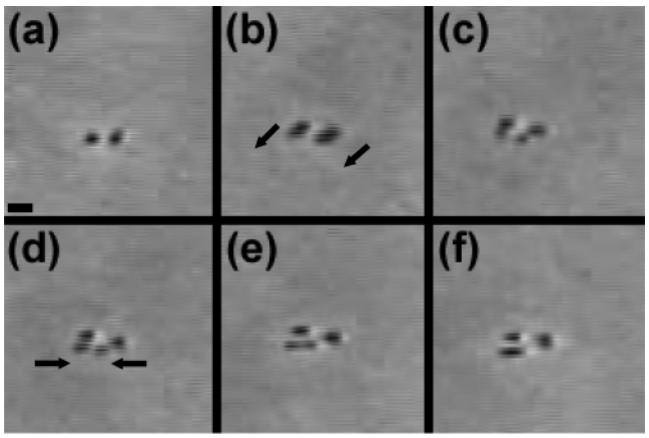

Figure 4. Phase contrast microscopy images of a simultaneous expulsion of two satellite vesicles from two initial vesicles followed by their fusion (A = 0.246 nm^2/molecule). Elapsed times are (a) 0, (b) 1.38, (c) 1.71, (d) 1.89, (e) 2.46, and (f) 3.18 s. The scale bar length is 10 μm.

to a direction (as shown with an arrow in Figure 7b) after the vesicle turns the direction of motion (Figure 7a). The rear part of the vesicle adheres to the original location on the monolayer and does not move to the direction that the front part of the vesicle moves during its extension. At the next step the rear part of the vesicle is detached from the monolayer and pulled forward to the front part (as shown with an arrow in Figure 7c), and during this process the front part is not pulled back (Figure 7d). The same sequence of extension, adhesion (de-adhesion), and retraction always governs throughout the directed motion (Figure 8). A typical trajectory of the vesicle that exhibits a directed motion is shown in Figure 9. The vectorial nature of the vesicle motion is clear.

Discussion

We have not studied the creation mechanism of vesicles here in any detail, but it is known that in general fluid liquid expanded (LE) monolayers such as those formed by phospholipids collapse via the ejection of material into the subphase by either molecular solubility or the formation of molecular aggregates such as vesicles or liposomes.[13] When a fatty acid is spread on an alkaline subphase as in this study, the polar, hydrophilic parts

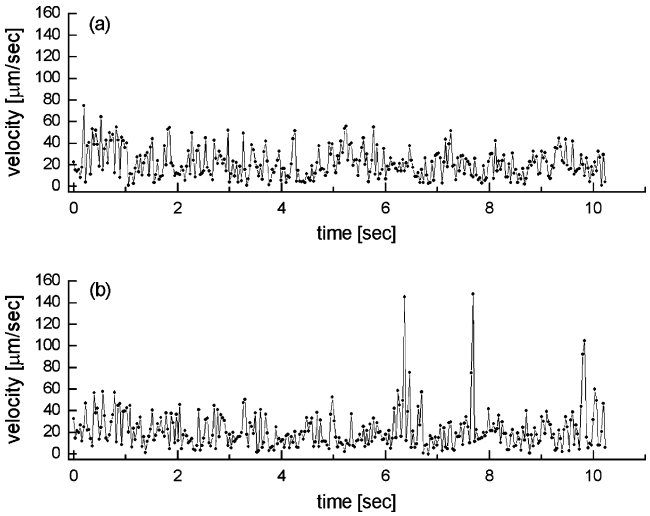

Figure 5. Two types of velocity profiles of self-propelled vesicles (0.243 nm^2/molecule). Note that the vesicle of type b shows definite intermittent velocity jumps between constant velocity fluctuations.

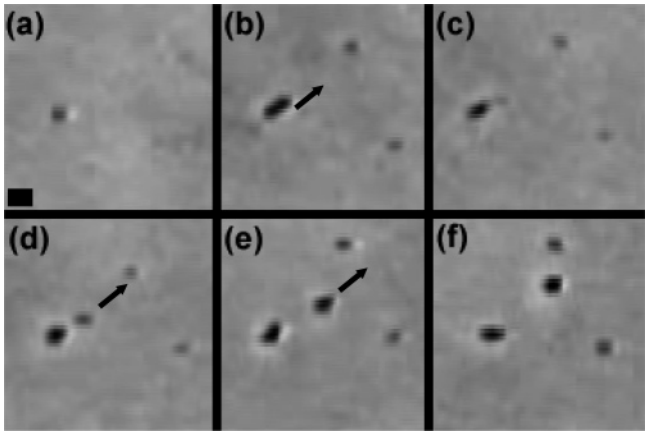

Figure 6. Phase contrast microscopy images to demonstrate a continuous motion of vesicle (A = 0.253 nm^2/molecule). Elapsed times are (a) 0, (b) 1.92, (c) 2.31, (d) 2.76, (e) 5.1, and (f) 7.98 s. The expelled vesicle spontaneously moves forward in a continuous manner. Note that the size of the expelled vesicle increases monotonically during the motion. The scale bar length is 10 μm.

are ionized. Such ionized films exhibit greatly enhanced solubility in water as compared with the corresponding uncharged monolayers. The solubilization will proceed more readily from LE monolayers than from liquid condensed (LC) ones, presumably because there is only a small energy barrier for the solution of molecules in the LE phase of a monolayer of stearic acid on water where the chain−chain interactions are comparatively weak in the monolayer, promoting molecules to dissolve into the bulk of the subphase. The appreciable solubilization of molecules into the bulk liquid phase in the LE phase may thus cause the creation of vesicles observed. Previous studies on collapse transitions in monophasic[13] and biphasic[5] monolayers suggested that the collapse mode depends strongly on the rheological properties (i.e., elasticity and fluidity) as well as cohesiveness of the monolayer at collapse. Giant folds and vesicles were found in disordered fluid LE monolayers.[5] Also in our study the viscoelastic nature of the solid monolayer was shown to affect its fracture mode dramatically.[9] Our present results demonstrate that on a buffered alkaline subphase the fatty acid monolayer becomes less cohesive to promote solubilization of material into the subphase, causing the creation of vesicles. The more rigid monolayer seems to adopt the selection of other collapse modes such as buckling, folding, and the formation of

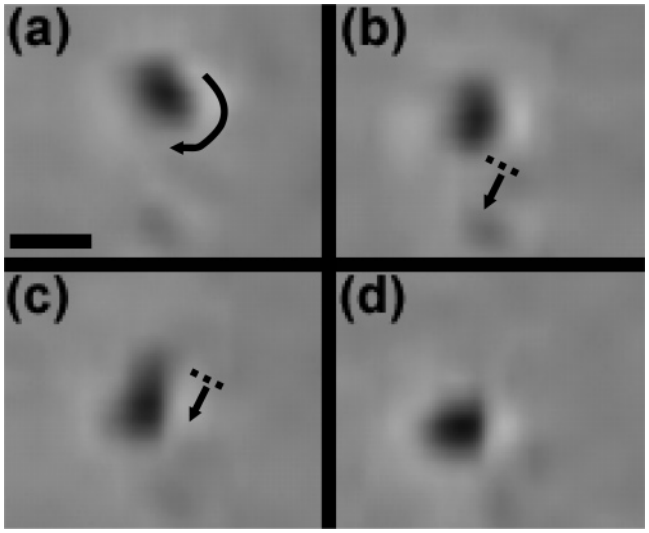

Figure 7. Phase contrast microscopy images to demonstrate an adhesion-mediated, self-propulsive motion of a vesicle ($A = 0.239$ nm^2/molecule). Elapsed times are (a) 0, (b) 0.03, (c) 0.07, and (d) 0.1 s. The motion of vesicle is characterized by vesicle *extension* followed by *adhesion* to the monolayer (b, c), and *retraction* of the rear part of the vesicle (d). The scale bar length is 10 μm.

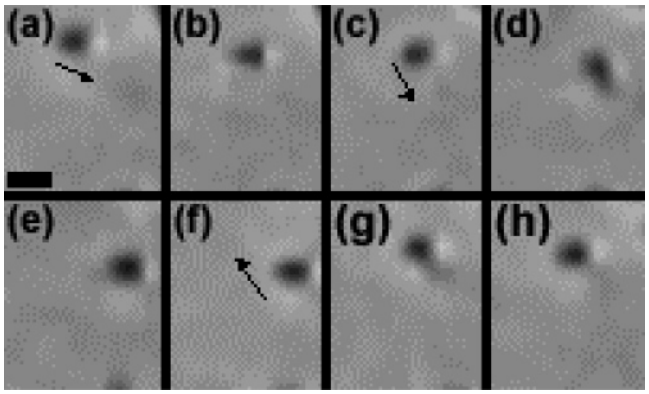

Figure 8. Long-time evolution of a self-propelled vesicle ($A = 0.24$ nm^2/molecule). Elapsed times are (a) 0, (b) 0.37, (c) 0.47, (d) 2.0, (e) 2.2, (f) 2.35, (g) 5.7, and (h) 6.37 s. The vesicle moves almost linearly and in both directions. Note that the vesicle always follows the same sequence (i.e., extension, adhesion, and retraction) to move in each direction. The scale bar length is 10 μm.

twisted ribbons on large length scales, since large-scale soft collapsed structures need moderate intensity of cohesiveness to keep their structures. A wide range of self-aggregation structures such as spherical micelles, lamellar bilayers, and helixes are known to form from simple long chain fatty acids. Single-chain, saturated, and unsaturated fatty acids were previously reported to form vesicles, which behave similarly in many respects to those formed from biological double-chain phospholipids.[14,15] Our results show that fatty acid vesicles are possible to form via a novel pathway, i.e., monolayer collapse. It is clear that the total volume of all vesicles upon vesicle division (Figures 2, 3, and 6) increases, suggesting that vesicle growth occurs by the incorporation of amphiphilic molecules into the existing vesicle membrane from the monolayer directly and/or via the bulk of subphase where the molecules are dissolved from the monolayer. This is also consistent with the fact that both the initial and the expelled vesicles are continuously fluctuating violently through the division event.

It is well-known that the imbalance in the adhesion force drives the biological cell to move directionally (haptotaxis[16,17]). The adhesive nature of the vesicle observed in this study

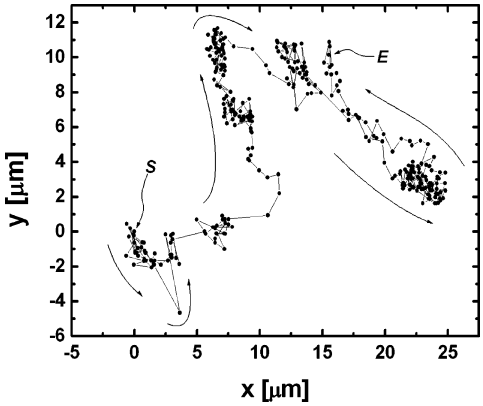

Figure 9. Typical trajectory of a self-propelled vesicle ($A = 0.242$ nm^2/molecule). The points denoted by the symbols *S* and *E* show initial and end points in the tracking of the motion of an active vesicle. The trajectory shows a directed motion with a velocity jump between random motions. The direction of motion is shown in arrows.

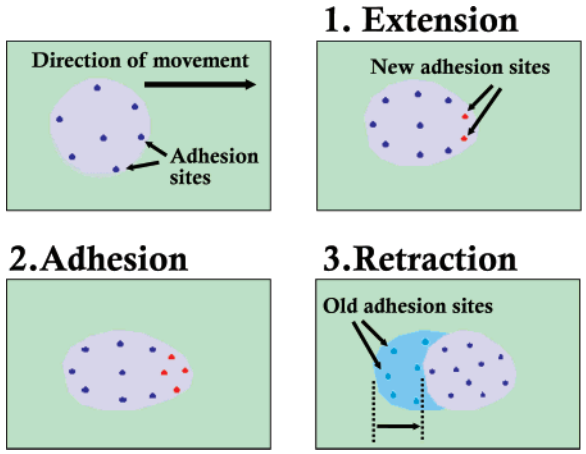

Figure 10. Cartoon of a self-propulsive motion of a fatty acid vesicle on a monolayer. The vesicle propels by three steps: (1) *extension* of the vesicle through new adhesion sites, (2) *adhesion* of the front part of extended vesicle, and (3) *retraction* of the vesicle by the de-adhesion of the rear part of the vesicle caused by tension between the front and the rear of the vesicle. Note that the existence of adhesion gradient of the monolayer to the vesicle is essential through the whole process of self-propulsion.

(Figures 7 and 8) is clear because if its advancing front does not adhere to the monolayer it will return to its original position like a free elastic body. The self-propelled, directed motion of vesicles observed is considered to be some adhesion-mediated process (Figure 10). The vesicle sticks out its front part to the monolayer, draws its rear part from the front, and finally reforms into the original shape at the new location selected by the front. The vesicle initiates the motion in the direction of the front part. We stress here that the vesicle moves forward not by "pushing from the back" but by "pulling from the front". Moderate intensity of adhesion force on the front part of the moving vesicle is required for such a motion to be possible, because if the adhesion force is too strong it will not move on the monolayer, while if it is too weak it will move continuously. A gradient in wettability can be produced either passively using surfaces with spatial variations in free energy or actively using chemical reactions with the surface that changes the wettability of the surface and induces a localized dewetting by the liquid. Since the latter reactive mechanical motion of the vesicle is based on the irreversible attachment of the adsorbates, we cannot expect the overlapping of the trajectory of motion generally.[18,19] We observed nevertheless that the vesicle moves forward and

backward and that its trajectory often crosses itself. Moreover, the increase of the total volume of vesicles before and after vesicle division is evident as described above. The adhesion gradient created by the local transfer of molecules between the vesicle and the monolayer is thus possible to activate the vesicle motion. This is consistent with the result that both the spontaneous motion and the shape fluctuation of vesicles cease with the decrease of the molecular area that makes the transfer of molecules difficult. The intermittent, adhesion-mediated directional motion of vesicle was observed more often at a late stage in a narrow molecular area range where vesicles were created, while at a larger molecular area the vesicle exhibited a continuous random motion only, indicating that the refinement of the intensity of the adhesion gradient of the monolayer to the vesicle allows one to observe the intermittent motion of a vesicle.

In the present study the adhesion between the vesicle and the supported monolayer is nonspecific (or electrostatic), compared to that in biological cell adhesion where it is mediated by specific ligand−receptor pairs. The phenomena we observed in this study are all nonequilibrium ones; hence, the vesicles move with velocities orders of magnitude faster than what is allowed by Brownian diffusion. We confined ourselves here to the case where vesicle propulsion is due to an adhesion gradient (haptotaxis). By using a simple dimensional argument, let us give a rough estimate of the adhesion energy difference on both sides of the vesicle on the substrate that provides the haptotactic power as the driving power of the moving vesicle. In a stationary regime where the vesicle acquires a constant drift velocity, by equating the driving power $P_{hapt} = L_{adh}\Delta w v$ (L_{adh}, the adhesion length; Δw, the difference in adhesion energy between the front and the rear of the vesicle; v, the constant drift velocity) due to the haptotactic force and the dissipation power $P_{hyd} = 6\pi\eta R v^2$ (η, the viscosity of water at room temperature; R, the vesicle radius) associated with the hydrodynamic friction, we obtain $\Delta w = 6\pi\eta R v/L_{adh}$. Putting $\eta = 10^{-3}$ Pa s (at 20 °C), $L_{adh} \sim 2R$, $R \sim 10$ μm, and $v \sim 10$ μm/s from our experiments, we get $\Delta w = 10^{-7}$ J/m^2 for the adhesion energy difference. This value lies in the range of theoretically predicted values ($\Delta w = 10^{-8}-10^{-6}$ J/m^2) in the weak adhesion regime.[20,21] If the adhesion energy w_f at the front of the vesicle is larger than w_r (the adhesion energy at the rear part), the vesicle must move in the direction of the front part. When $w_f = w_r$ and equilibrium is reached on a homogeneous substrate, one expects a vanishing velocity of the moving vesicle. The slowest dissipation mechanism will limit the motion. In the vesicle propulsion dissipation generally occurs both in the surrounding fluid and in the membrane. Dissipation within the membrane becomes relevant only at shorter length scales or equivalently faster time scales. Membrane viscosity due to friction between the two monolayers becomes relevant in the submicron range. On smaller scales of several tenths of nanometers, shear viscosity within each layer should be included. For vesicles on scales of microns and larger as in our case, the dominant dissipation is hydrodynamic dissipation in the surrounding fluid.[22] We consider the situation where hydrodynamic, viscous dissipation is the limiting factor and restrict ourselves to nondissipative adhesion because we are in a position to consider the nonspecific adhesion in this study. Roughly, we can check the order of magnitude of the relaxation time τ_{hapt} of the vesicle propulsion by combining the hydrodynamic friction and the haptotactic force, $6\pi\eta R(L_{adh}/\tau_{hapt}) \sim L_{adh}\Delta w$; then we get $\tau_{hapt} \sim 6\pi\eta R/\Delta w \sim 1$ s. We can compare the time scale τ_{hapt} with the relaxation time of an isolated fluctuating membrane, τ_{fluc}, which is given by $\tau_{fluc} \sim \eta R^3/\kappa \sim$ 10 s, where κ is the bending rigidity ($\kappa \sim 20k_BT$).[22] In this relaxation process, the driving force due to the bending rigidity is balanced by the hydrodynamic frictional force characterized by the viscosity of the surrounding fluid. Comparing the two time scales, one finds that the difference of the time scales is not so remarkable. One may thus expect that haptotactic motions and membrane fluctuations are dynamically coupled to each other. In fact, the haptotactic motion of the vesicle was accompanied by strong shape fluctuations in our experiments generally. We note that shape fluctuation is a key factor for the initiation of vesicle propulsion due to haptotaxis through nonspecific interactions, because it causes a local contact between the vesicle and the supported monolayer, inducing an adhesion gradient on the substrate through local charge neutralization at the contact region.

Conclusions

We have observed a variety of spontaneous motions of vesicles under the nonequilibrium condition that molecular transfer is possible between the vesicle and the supported monolayer. The behaviors of vesicles are biological cell-like ones such as division, fusion, and migration. The migration of vesicles along the monolayer is a complex adhesion-mediated process, involving extension, adhesion, and retraction. These processes require the traction forces arising from adhesion gradients for the vesicle to be exerted on the monolayer and vesicle contractility. The adhesion gradients are created by the local transfer of molecules between the vesicle and the supported monolayer. The vanishing molecular transfer between them due to the decrease of the molecular area leads to the loss of the adhesion gradients, preventing vesicles from moving spontaneously.

References and Notes

(1) Ries, H. E., Jr.; Swift, H. W. *Langmuir* **1987**, *3*, 853.
(2) Hatta, E.; Hosoi, H.; Akiyama, H.; Ishii, T.; Mukasa, K. *Eur. Phys. B* **1998**, *2*, 347.
(3) Stine, K. J.; Knobler, C. M.; Desai, R. C. *Phys. Rev. Lett.* **1980**, *65*, 1004.
(4) Diamant, H.; Witte, T. A.; Gopal, A.; Lee, K. Y. C. *Europhys. Lett.* **2000**, *28*, 565.
(5) Gopal, A.; Lee, K. Y. C. *J. Phys. Chem. B* **2001**, *105*, 10348.
(6) Ybert, C.; Lu, W.; Moller, G.; Knobler, C. M. *J. Phys. Chem. B* **2002**, *106*, 2004.
(7) Lu, W.; Knobler, C. M.; Bruinsma, R. F.; Twardos, M.; Dennin, M. *Phys. Rev. Lett.* **2002**, *89*, 146107.
(8) Pauchard, L.; Meunier, J. *Phys. Rev. Lett.* **1993**, *70*, 3565.
(9) Hatta, E.; Suzuki, D.; Nagao, J. *Eur. Phys. J. B* **1999**, *11*, 609. Hatta, E.; Fischer, Th. M. *J. Phys. Chem. B* **2002**, *106*, 589.
(10) Boal, D. H. *Mechanics of the Cell*; Cambridge University Press: Cambridge, U.K., 2002.
(11) Nelson, P.; *Biological Physics: Energy, Information, Life*; W. H. Freeman: New York, 2003.
(12) Cooper, G. M.; Hausman, R. E. *The Cell: A Molecular Approach, 4th ed.*; Sinauer Associates: Sunderland, MA, or Cambridge University Press: Cambridge, U.K., 2007.
(13) Lipp, M. M.; Lee, K. Y. C.; Takamoto, D. Y.; Zasadzinski, J. A.; Waring, A. J. *Phys. Rev. Lett.* **1998**, *81*, 1650.
(14) Gebicki, J. M.; Hicks, M. *Nature* **1973**, *243*, 232. Gebicki, J. M.; Hicks, M. *Chem. Phys. Lipids* **1976**, *16*, 142.
(15) Hargreaves, W. R.; Deamer, D. W. *Biochemistry* **1980**, *17*, 3759.
(16) Carter, S. B. *Nature* **1967**, *213*, 256.
(17) Solon, J.; Streicher, P.; Richter, R.; Brochard-Wyart, F.; Bassereau, P. *Proc. Natl. Acad. Sci. U.S.A.* **2006**, *103*, 12387.
(18) Chaudhury, M. K.; Whitesides, G. M. *Science* **1992**, *256*, 1539.
(19) Bain, C. D.; Burnett-Hall, G. D.; Montgomerie, R. R. *Nature* **1994**, *372*, 414.
(20) Cantat, I.; Misbah, C. *Phys. Rev. Lett.* **1999**, *83*, 235.
(21) Tordeux, C.; Fournier, J.-B.; Galatola, P. *Phys. Rev. E* **2002**, *65*, 041912.
(22) Brochard, F.; Lennon, J. F. *J. Phys.* **1975**, *36*, 1035.